GEOPHYSICAL RESEARCH LETTERS, VOL. 40, 5268–5273, doi:10.1002/grl.50927, 2013

A practical method to identify displaced and split stratospheric polar vortex events

William J. M. Seviour,[1] Daniel M. Mitchell,[1,2] and Lesley J. Gray[1,2]

Received 1 July 2013; revised 2 September 2013; accepted 4 September 2013; published 1 October 2013.

[1] Extreme variability of the stratospheric polar vortex during winter can manifest as a displaced vortex event or a split vortex event. The influence of this vortex disruption can extend downwards and affect surface weather patterns. In particular, vortex splitting events have been associated with a negative Arctic Oscillation pattern. An assessment of the impacts of climate change on the polar vortex is therefore important, and more climate models now include a well-resolved stratosphere. To aid this analysis, we introduce a practical threshold-based method to distinguish between displaced and split vortex events. It requires only geopotential height at 10 hPa to measure the geometry of the vortex using two-dimensional moment diagnostics. It captures extremes of vortex variability at least, as well as previous methods when applied to reanalysis data, and has the advantage of being easily employed to analyze climate model simulations. **Citation:** Seviour, W. J. M., D. M. Mitchell, and L. J. Gray (2013), A practical method to identify displaced and split stratospheric polar vortex events, *Geophys. Res. Lett.*, *40*, 5268–5273, doi:10.1002/grl.50927.

1. Introduction

[2] A well-resolved stratosphere is now included in many operational forecast, seasonal prediction, and climate models [*Gerber et al.*, 2012], and it is becoming increasingly important to develop improved diagnostics of stratospheric variability. The stratosphere is of particular interest for modeling groups because of the established link between variability of the stratospheric polar vortex and anomalous weather patterns at the Earth's surface [e.g., *Baldwin and Dunkerton*, 2001]. This link is particularly strong following extreme events known as stratospheric sudden warmings (SSWs), in which the strong westerly winds that usually dominate the winter polar stratosphere become highly disturbed (here, for reasons outlined below, we use the term SSW to encompass a wider range of variability than its traditional definition). These events have been linked to a shift in the midlatitude storm tracks [*Thompson and Wallace*, 2001], an increase in high-latitude blocking events [*Woollings et al.*, 2010], and an increased chance of cold spells over northern Europe [*Tomassini et al.*, 2012]. Making use of these relationships, it has been demonstrated that knowledge of the stratosphere is of benefit for extended-range weather forecasting [*Baldwin et al.*, 2003] and climate projections [*Scaife et al.*, 2012; *Hardiman et al.*, 2012].

[3] Traditional methods to identify SSWs have relied on either zonal mean [*Andrews et al.*, 1987] or annular mode [*Baldwin and Dunkerton*, 2001] diagnostics. Neither method explicitly deals with the inherent zonal asymmetry in vortex variability. In particular, SSWs are observed to occur in one of two manners: displaced vortex events, where the vortex moves far from the pole, and split vortex events, where the vortex divides into two separate vortices. These two types have a very different spatial structure and evolution timescale [*Matthewman et al.*, 2009]. Displaced and split vortex events are predominantly associated with vertically propagating Rossby waves of wave numbers 1 and 2 respectively, and many previous studies have classified SSWs based on wave number [e.g., *Nakagawa and Yamazaki*, 2006]. However, this method does not provide a description of the location of the polar vortex itself, which theoretical arguments suggest may be important for understanding stratosphere-troposphere coupling [*Ambaum and Hoskins*, 2002]. In an improvement to these traditional SSW definitions, *Charlton and Polvani* [2007] (hereafter CP07) introduced a classification in which a split vortex event is identified when two vortices with a circulation ratio of 2:1 or higher are present, and all other SSWs are automatically classed as displaced vortex events. However, they maintained the traditional SSW identification which requires there to be a reversal of the zonal-mean zonal wind at 10 hPa and 60°N.

[4] An increased understanding of stratospheric variability can be gained by using vortex-centric diagnostics, such as two-dimensional (2-D) vortex moments [*Waugh*, 1997; *Waugh and Randel*, 1999; *Mitchell et al.*, 2011a, 2011b], which provide a geometrical description of the vortex and have no reliance on zonal-mean properties. Using a classification based on these diagnostics, *Mitchell et al.* [2013] (hereafter M13) identified a greater number of SSWs than CP07. This is primarily because they did not use a zonal-mean threshold criterion. Importantly, M13 also demonstrated that split vortex events penetrated deep into the troposphere and resulted in significant surface anomalies, while anomalies associated with displaced vortex events do not descend far below the tropopause. Their result supported a similar conclusion by *Nakagawa and Yamazaki* [2006], who found that the impact of events associated with an enhanced upward flux of wave number-2 planetary waves was more likely to reach the surface. In contrast, *Cohen and Jones* [2011] found that surface anomalies were similar following the split and displaced vortex events defined by CP07, but there were significant

Additional supporting information may be found in the online version of this article.

[1]Department of Physics, University of Oxford, Oxford, UK.
[2]National Centre for Atmospheric Science, University of Oxford, Oxford, UK.

Corresponding author: W. J. M. Seviour, University of Oxford, Oxford, UK. (seviour@atm.ox.ac.uk)

0094-8276/13/10.1002/grl.50927

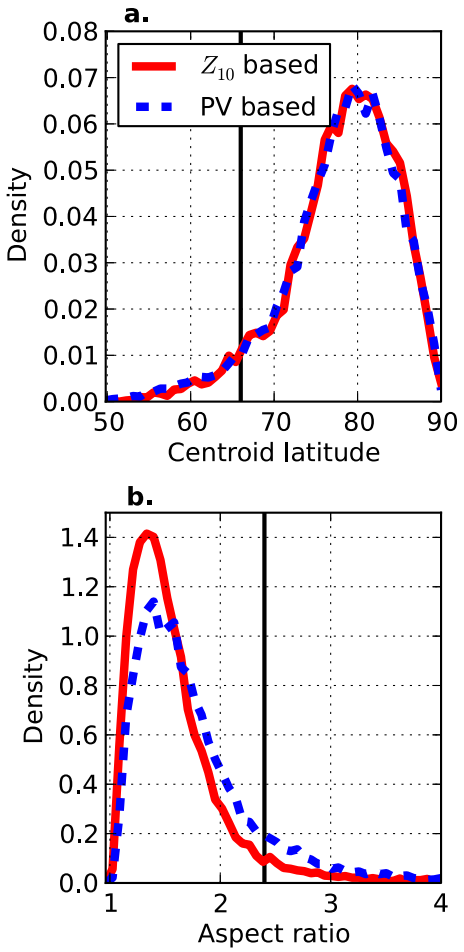

Figure 1. Distributions of the December–March (a) centroid latitude and (b) aspect ratio of the Northern Hemisphere stratospheric polar vortex over 1958–2009. Diagnostics are calculated from geopotential height at 10 hPa (Z_{10}) and potential vorticity at 850 K (PV). Thresholds of 66°N in centroid latitude and 2.4 in aspect ratio are used to define events and are indicated by the solid vertical lines.

differences in the tropospheric precursors. These results underline the need to correctly identify the precise type of SSW, in order to understand stratosphere-troposphere coupling within climate models.

[5] Distinguishing between displaced and split vortex events using the method of M13 requires the use of potential vorticity (PV), which is not commonly output by climate models. For this reason, previous attempts to apply PV-based techniques in a multimodel study have led to the majority of models being excluded [*Mitchell et al.*, 2012]. Furthermore, their method used a hierarchical clustering technique [*Hannachi et al.*, 2010], which is very sensitive to the exact shape of the distribution of vortex variability, so is unsuitable for application to a range of models with different climatologies. In this study, we develop an improved method which (a) is based on the geometry of the vortex, but requires only the 10 hPa geopotential height, and (b) identifies events using a simple threshold instead of a clustering technique. We apply this new method to the ERA-40 and ERA-Interim reanalysis data sets and demonstrate that the method captures a similar number of events which are in good agreement with, and at least as extreme as, those of M13.

2. The Z_{10} Method

2.1. Vortex Geometry Calculation

[6] Northern Hemisphere winter daily-mean data for December–March (DJFM) were employed. The European Centre for Medium-Range Weather Forecasts ERA-40 data set [*Uppala et al.*, 2005] is used from 1958 to 1979 and ERA-Interim [*Dee et al.*, 2011] from 1979 to 2009. The geometry of the vortex is described in terms of the latitude of the center of the vortex (centroid latitude) and aspect ratio (a measure of how stretched the vortex is).

[7] The method calculates the 2-D vortex moment of order $a + b$, defined in Cartesian coordinates as

$$\mu_{ab} = \iint_S [X(x,y) - \bar{X}] x^a y^b \mathrm{d}x\mathrm{d}y \,, \qquad (1)$$

where $\bar{X}$ is a single contour of PV or geopotential height, representing the vortex edge. The value of this contour is

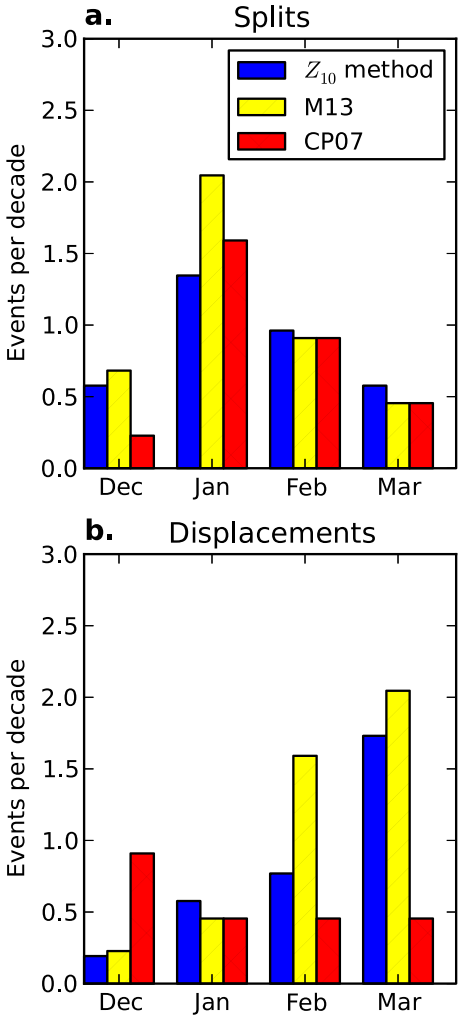

Figure 2. Histogram of the seasonal distribution of (a) split and (b) displaced vortex events forms the Z_{10} method, M13, and CP07.

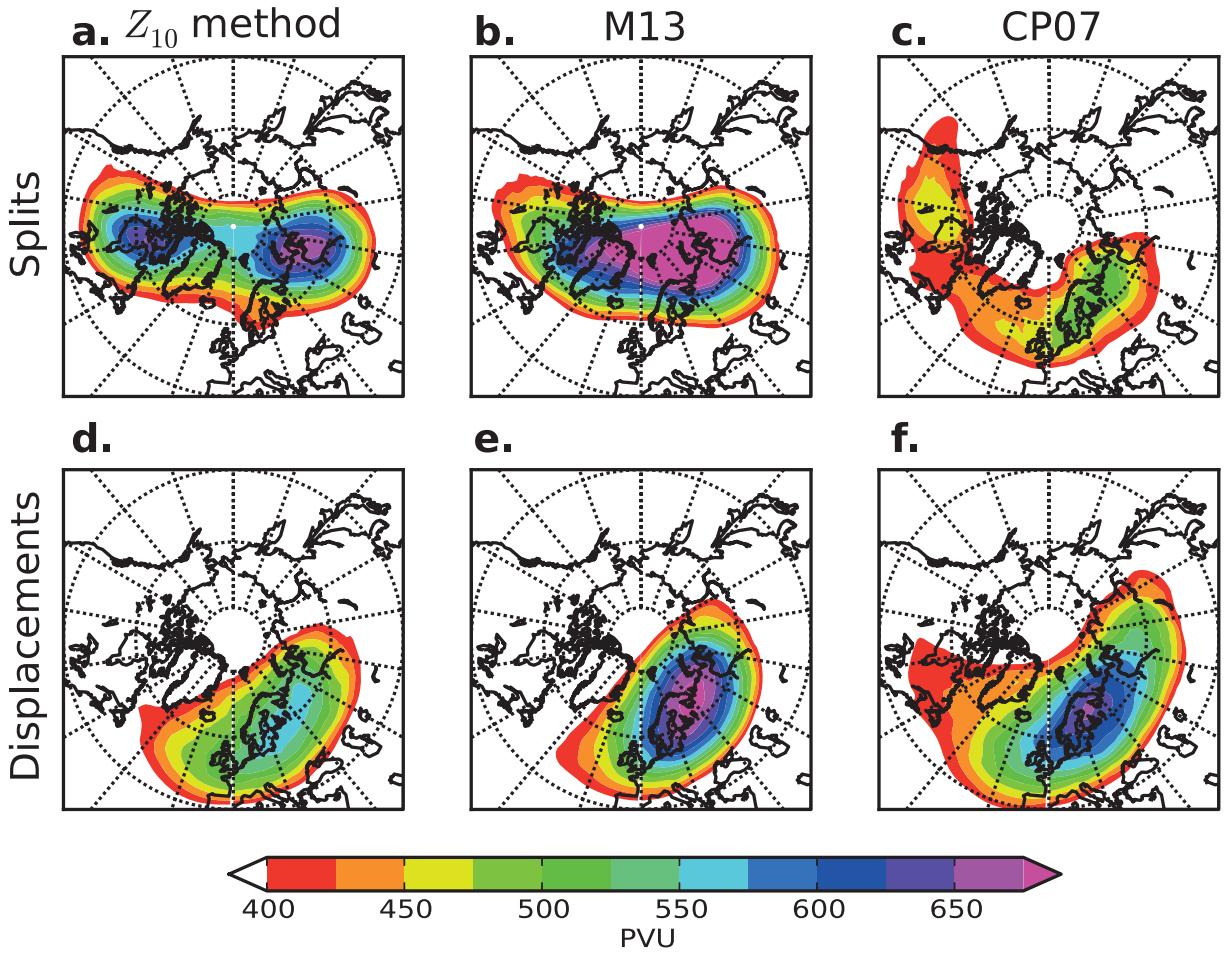

Figure 3. Composites of potential vorticity at the 850 K isentropic surface. Composites are taken over the 5 days following the onset date of (a, b, c) split vortex events and 7 days following (d, e, f) displaced vortex events (the difference is due to the different timescales of these events). We compare the current (Z_{10}) method (Figures 3a and 3d) with that of M13 (Figures 3b and 3e) and CP07 (Figures 3c and 3f).

chosen to match that of the 10 hPa geopotential height (Z_{10}) or 850 K PV (PV_{850}) DJFM zonal mean at 60°N (however, the results are not sensitive to the exact choice of contour between about 50° and 70°N). Following the method of *Matthewman et al.* [2009] (to which readers are referred for technical details), equation (1) allows for the explicit calculation of the centroid latitude and aspect ratio on a particular pressure level or isentropic surface. Other moment diagnostics can be extracted, such as vortex area and kurtosis, but these were not found necessary for identifying split and displaced vortex events, and are therefore omitted from the analysis.

[8] Figure 1 compares the distribution of aspect ratio and centroid latitude, calculated using daily PV_{850} and Z_{10}. The centroid latitude distributions are almost identical, with a peak around 80°N. The aspect ratio distributions have a similar shape, with a peak at about 1.3, but the PV-based diagnostic has a larger tail. This is to be expected, since the PV field contains more small-scale, filamentary structures than geopotential height. Neither distribution shows bimodality, suggesting that the application of clustering techniques, as in *Coughlin and Gray* [2009] and *Hannachi et al.* [2010], may be inappropriate. As well as having similar distributions, the time series of the PV and geopotential height-derived diagnostics (not shown) are well correlated, with correlation coefficients of 0.9 for centroid latitude and 0.6 for aspect ratio.

2.2. Event Definition

[9] In order to identify displaced and split vortex events, a threshold criterion is introduced and applied to the geopotential height derived diagnostics. A displaced vortex event requires the centroid latitude to remain equatorward of 66°N for 7 days or more. A split vortex event requires the aspect ratio to remain higher than 2.4 for 7 days or more. These thresholds are indicated in Figure 1, and were selected to give a similar frequency of displacement and splitting events as M13. They capture the 5.7% most equatorward values of centroid latitude, and the largest 5.2% of aspect ratio values. This choice is somewhat subjective, but the results presented below are not sensitive to the exact choice of threshold. There were no occasions on which both criteria were met simultaneously. The onset date is defined as the day that the appropriate threshold is first exceeded, and to ensure that no events are counted twice, the events are required to be spaced at least 30 days apart, chosen to reflect radiative timescales in the lower stratosphere [*Newman and Rosenfield*, 1997]. *Mitchell et al.* [2011a] found that the

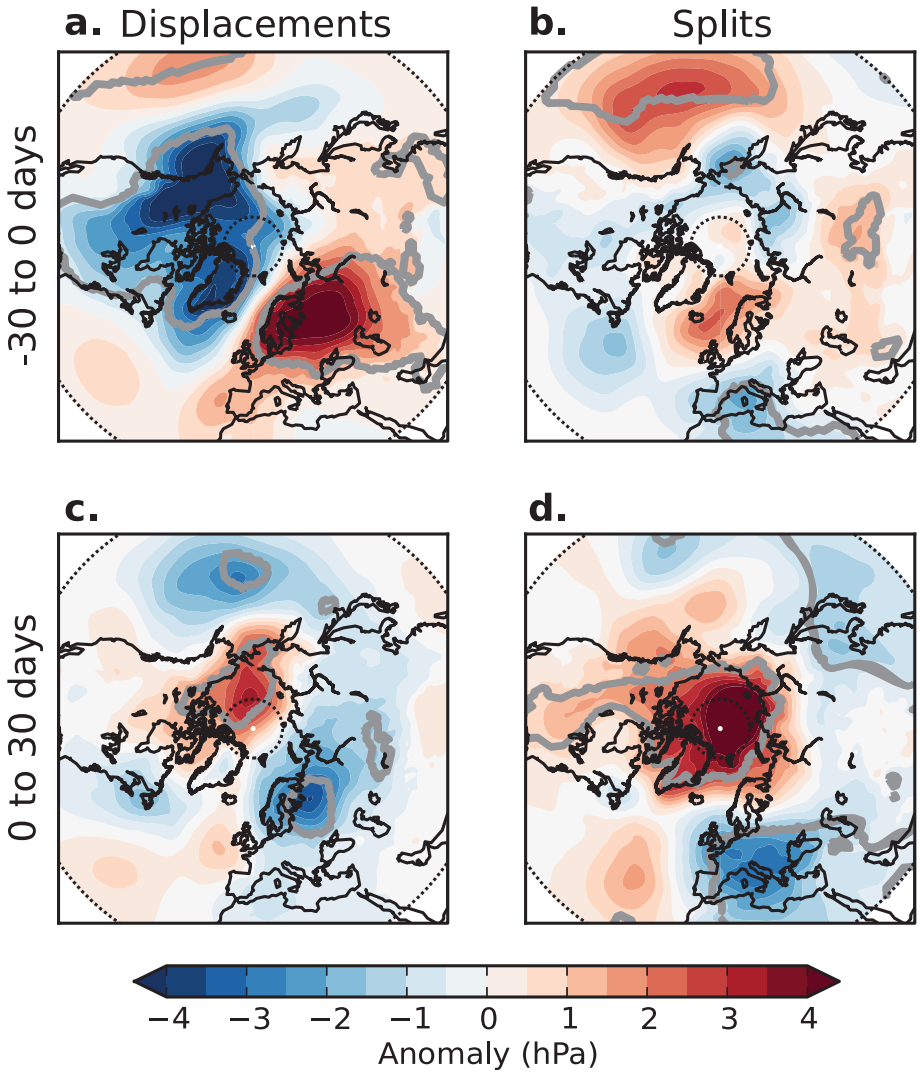

Figure 4. Composites of mean sea-level pressure anomalies in the (a and b) 30 days before and (c and d) 30 days after the onset dates of displaced (Figures 4a and 4c) and split (Figures 4b and 4d) vortex events from the Z_{10} method. Anomalies are calculated for each day and grid point from the climatology for that day of the year and grid point. Grey contours indicate regions of greater than 95% statistical significance according to a Monte Carlo significance test.

aspect ratio and centroid latitude follow an extreme value distribution [*Coles*, 2001] and we note that both thresholds chosen here lie beyond the extreme value thresholds of their respective distributions. Using this method, 17 displaced and 18 split vortex events (listed in Table S1 in the supporting information) are identified over the 52 winters, an average of 7 per decade. These events are all midwinter events – the DJFM data were used explicitly to avoid counting final warmings. This frequency lies between the values of CP07 (6/decade) and M13 (8/decade).

[10] There are significant differences in the seasonal distribution of displaced and split vortex events, as shown in Figure 2. Split vortex events are more frequent in early-mid winter, with a peak in January, while displaced vortex events are skewed towards late winter. Figure 2 also shows the seasonal distribution of displaced and split vortex events from CP07 and M13. The shape of the distribution agrees well with the seasonal distribution found by M13 for both types of event. However, there is less similarity with the CP07 distribution of displaced vortex events (Figure 2b). CP07 indicates an approximately flat distribution throughout winter, and many fewer displaced vortex events overall. It should be noted that the seasonal distribution of displaced and split vortex events from the moment based methods does not arise from the underlying climatology of centroid latitude or aspect ratio, which remains approximately constant throughout winter [*Mitchell et al.*, 2011a]. As well as better agreement with M13 than with CP07 in the seasonal distribution of displaced vortex events, there is also a better match in the identification of individual events (Table S2 in the supporting information).

3. Analysis

[11] To evaluate how well the new method captures displaced and split vortex events, Figure 3 shows composites of PV in the midstratosphere (850 K) following their onset dates. These are averaged over the 5 days following the onset date for split events and 7 days for displaced events (these averaging periods reflect the different timescales of

the events). The composites are compared with the corresponding composites following the events identified by M13 and CP07. For the split vortex events, the Z_{10} method clearly shows two separated vortices, one centered over Canada and the other over Siberia. This characteristic direction reflects the climatological wave-2 pattern at this altitude. For the M13 events, the split vortex composite shows the vortex stretched across the same 90°W–90°E line, although not as clearly split, while the composite for the CP07 events looks very different. This has a weak vortex centered over Canada, with the other over Northern Europe, and is similar to the composite for displaced events. All three composites for displaced events show a vortex centered over Northern Europe, but this extends most westward in the CP07 composite, suggesting that there may be some contamination from misdiagnosed split vortex events.

[12] Figure 3 demonstrates that the Z_{10} method succeeds in identifying displaced and split vortex events at least, as well as the methods of M13 or CP07. When comparing the three methods, CP07 is the clear outlier. This is most likely because both the Z_{10} method and M13 use a fully 2-D approach, while CP07 employ the traditional zonal-mean threshold which cannot accurately capture the extreme events.

[13] M13 found that the mean sea-level pressure (MSLP) anomalies are different before and after displaced and split vortex events. In Figure 4, we present composites of MSLP 30 days before and 30 days following the onset dates of displaced and split vortex events, calculated using the Z_{10} method. Statistical significance is estimated from a Monte Carlo method, using 10^5 composites of equal size, formed from randomly sampled winter dates.

[14] The strongest precursor is found for displaced vortex events, with a wave-1 pattern that is similar to the stationary wave pattern [e.g., *Garfinkel and Hartmann*, 2008], suggesting increased wave-1 propagation into the stratosphere. However, the strongest anomalies following events occur after split vortex events. The main features of Figure 4 compare very well with the corresponding diagnostics from M13, confirming the accuracy of the new method.

4. Summary

[15] Recent research has demonstrated the need to distinguish between displaced and split stratospheric polar vortex events due to their different impacts on surface weather patterns. However, current methods to identify these events are complex or require nonstandard variables. In this paper, a new, robust method has been developed to identify displaced and split vortex events, which requires only geopotential height at 10 hPa. The method is briefly summarized as follows.

[16] 1. To identify the vortex region, a single contour of 10 hPa geopotential height is selected: the value of the zonal mean at 60°N.

[17] 2. Using this contour and the geopotenial height field, the centroid latitude and aspect ratio are calculated, following the methodology of *Matthewman et al.* [2009].

[18] 3. Events are identified using a threshold criterion: Displaced events are identified if the centroid latitude remains equatorward 66°N for 7 days or more. Split events are identified if the aspect ratio remains above 2.4 for 7 days or more. No two events may occur within 30 days.

[19] It is important to note that this method relies on a time mean state in selecting the contour. While this allows for the correction of biases in the mean state of models, it may lead to the reclassification of past events as the mean state changes under a changing climate (although results are not highly sensitive to the exact location of the contour). This difficulty may be overcome by allowing the mean state to evolve slowly in time, as suggested by *Gerber et al.* [2010]. The method also relies on a persistence criterion which prohibits events being identified in real time, as may be desired by early warning systems for SSWs such as STRATALERT [*Labitzke and Naujokat*, 2000]. However, despite this persistence criterion, the majority of events defined by this method are identified before corresponding events under the traditional definition, and it may be possible to use instantaneous values with larger thresholds if real time identification is required.

[20] Nevertheless, results using this method demonstrate that it is able to identify splitting and displacement events at least as effectively as previous methods. It reproduces the different surface anomalies before and after displaced and split vortex events, as identified by M13. This reinforces the conclusion of M13 that it is important to distinguish between displaced and split vortex events when assessing the impact of winter stratospheric variability on surface climate.

[21] **Acknowledgments.** WJMS and DMM are supported by a grant from the UK Natural Environment Research Council (NERC). LJG is funded by the NERC National Centre for Atmospheric Science (NCAS). We are grateful for the constructive comments and suggestions of an anonymous reviewer.

[22] The Editor thanks one anonymous reviewer for his/her assistance in evaluating this paper.

References

Ambaum, M. H. P., and B. J. Hoskins (2002), The NAO troposphere-stratosphere connection, *J. Climate*, *15*, 1969–1978.

Andrews, D., J. R. Holton, and C. Leovy (1987), *Middle Atmosphere Dynamics,* 489 pp., Academic Press, San Diego, Calif.

Baldwin, M. P., and T. J. Dunkerton (2001), Stratospheric harbingers of anomalous weather regimes, *Science*, *294*, 581–584, doi:10.1126/science.1063315.

Baldwin, M. P., D. B. Stephenson, D. W. J. Thompson, T. J. Dunkerton, A. J. Charlton, and A. O'Neill (2003), Stratospheric memory and skill of extended-range weather forecasts, *Science*, *301*, 636–640, doi:10.1126/science.1087143.

Charlton, A. J., and L. M. Polvani (2007), A new look at stratospheric sudden warmings. Part I: Climatology and modeling benchmarks, *J. Climate*, *20*, 449–469, doi:10.1175/JCLI3996.1.

Cohen, J., and J. Jones (2011), Tropospheric precursors and stratospheric warmings, *J. Climate*, *24*, 6562–6572, doi:10.1175/2011JCLI4160.1.

Coles, S. (2001), *An Introduction to Statistical Modeling of Extreme Values,* 209 pp., Springer, London.

Coughlin, K., and L. J. Gray (2009), A continuum of sudden stratospheric warmings, *J. Atmos. Sci.*, *66*, 531–540, doi:10.1175/2008JAS2792.1.

Dee, D. P., et al. (2011), The ERA-Interim reanalysis: Configuration and performance of the data assimilation system, *Q. J. R. Meteorol. Soc.*, *137*(656), 553–597, doi:10.1002/qj.828.

Garfinkel, C. I., and D. L. Hartmann (2008), Different ENSO teleconnections and their effects on the stratospheric polar vortex, *J. Geophys. Res.*, *113*, D18114, doi:10.1029/2008JD009920.

Gerber, E. P., et al. (2010), Stratosphere-troposphere coupling and annular mode variability in chemistry-climate models, *J. Geophys. Res.*, *115*, D00M06, doi:10.1029/2009JD013770.

Gerber, E. P., A. Butler, N. Calvo, A. J. Charlton-Perez, M. Giorgetta, E. Manzini, and J. Perlwitz (2012), Assessing and understanding the impact of stratospheric dynamics and variability on the earth system, *Bull. Am. Meteorol. Soc.*, *93*, 845–859, doi:10.1175/BAMS-D-11-00145.1.

Hannachi, A., D. M. Mitchell, L. J. Gray, and A. Charlton-Perez (2010), On the use of geometric moments to examine the continuum of sudden stratospheric warmings, *J. Atmos. Sci.*, *68*, 657–674, doi:10.1175/2010JAS3585.1.

Hardiman, S. C., N. Butchart, T. J. Hinton, S. M. Osprey, and L. J. Gray (2012), The effect of a well-resolved stratosphere on surface climate: Differences between CMIP5 simulations with high and low top versions of the met office climate model, *J. Climate*, *25*, 7083–7099, doi:10.1175/JCLI-D-11-00579.1.

Labitzke, K., and B. Naujokat (2000), *The Lower Arctic Stratosphere Since 1952, SPARC Newsletter, No. 15*, SPARC Office, Toronto, ON, Canada.

Matthewman, N. J., J. G. Esler, A. J. Charlton-Perez, and L. M. Polvani (2009), A new look at stratospheric sudden warmings. Part III: Polar vortex evolution and vertical structure, *J. Climate*, *22*, 1566–1585, doi:10.1175/2008JCLI2365.1.

Mitchell, D. M., A. J. Charlton-Perez, and L. J. Gray (2011a), Characterizing the variability and extremes of the stratospheric polar vortices using 2D moment analysis, *J. Atmos. Sci.*, *68*, 1194–1213, doi:10.1175/2010JAS3555.1.

Mitchell, D. M., L. J. Gray, and A. J. Charlton-Perez (2011b), The structure and evolution of the stratospheric vortex in response to natural forcings, *J. Geophys. Res.*, *116*, D15110, doi:10.1029/2011JD015788.

Mitchell, D. M., et al. (2012), The nature of Arctic polar vortices in chemistry-climate models, *Q. J. R. Meteorol. Soc.*, *138*, 1681–1691, doi:10.1002/qj.1909.

Mitchell, D. M., L. J. Gray, J. Anstey, M. P. Baldwin, and A. J. Charlton-Perez (2013), The influence of stratospheric vortex displacements and splits on surface climate, *J. Climate*, *26*, 2668–2682, doi:10.1175/JCLI-D-12-00030.1.

Nakagawa, K. I., and K. Yamazaki (2006), What kind of stratospheric sudden warming propagates to the troposphere?, *Geophys. Res. Lett.*, *33*, L04801, doi:10.1029/2005GL024784.

Newman, P., and J. Rosenfield (1997), Stratospheric thermal damping times, *Geophys. Res. Lett.*, *24*, 433–436, doi:10.1029/96GL03720.

Scaife, A. A., et al. (2012), Climate change projections and stratosphere-troposphere interaction, *Clim. Dyn.*, *38*, 2089–2097, doi:10.1007/s00382-011-1080-7.

Thompson, D. W., and J. M. Wallace (2001), Regional climate impacts of the Northern Hemisphere annular mode, *Science*, *293*, 85–9, doi:10.1126/science.1058958.

Tomassini, L., E. P. Gerber, M. P. Baldwin, F. Bunzel, and M. Giorgetta (2012), The role of stratosphere-troposphere coupling in the occurrence of extreme winter cold spells over northern Europe, *J. Adv. Model. Earth. Syst.*, *4*, M00A03, doi:10.1029/2012MS000177.

Uppala, S. M., et al. (2005), The ERA-40 re-analysis, *Q. J. R. Meteorol. Soc.*, *131*(612), 2961–3012, doi:10.1256/qj.04.176.

Waugh, D. W. (1997), Elliptical diagnostics of stratospheric polar vortices, *Q. J. R. Meteorol. Soc.*, *123*, 1725–1748, doi:10.1002/qj.49712354213.

Waugh, D. W., and W. J. Randel (1999), Climatology of arctic and antarctic polar vortices using elliptical diagnostics, *J. Atmos. Sci.*, *56*, 1594–1613.

Woollings, T., A. Charlton-Perez, S. Ineson, A. G. Marshall, and G. Masato (2010), Associations between stratospheric variability and tropospheric blocking, *J. Geophys. Res.*, *115*, D06108, doi:10.1029/2009JD012742.